Master's Thesis
석사 학위논문

Improvement of Target Registration Accuracy with Anatomical Landmarks

Jaeyeong Park（박 재 영 朴 在 泳）

Department of Robotics Engineering
로봇공학전공

DGIST

2013

Master's Thesis
석사 학위논문

Improvement of Target Registration Accuracy with Anatomical Landmarks

Jaeyeong Park（박 재 영 朴 在 泳）

Department of Robotics Engineering
로봇공학전공

DGIST

2013

Improvement of Target Registration Accuracy with Anatomical Landmarks

Advisor : Professor Jaesung Hong

Co-advisor : Professor Jeon Il Moon

By

Jaeyeong Park
Department of Robotics Engineering
DGIST

A thesis submitted to the faculty of DGIST in partial fulfillment of the requirements for the degree of Master of Science in the Department of Robotics Engineering. The study was conducted in accordance with Code of Research Ethics[1]

01. 03. 2013

Approved by

Professor Jaesung Hong (Advisor) (Signature)

Professor Jeon Il Moon (Co-Advisor) (Signature)

[1] Declaration of Ethical Conduct in Research: I, as a graduate student of DGIST, hereby declare that I have not committed any acts that may damage the credibility of my research. These include, but are not limited to: falsification, thesis written by someone else, distortion of research findings or plagiarism. I affirm that my thesis contains honest conclusions based on my own careful research under the guidance of my thesis advisor.

Improvement of Target Registration Accuracy with Anatomical Landmarks

Jaeyeong Park

Accepted in partial fulfillment of the requirements for the degree of Master of Science.

12. 03. 2012

Head of Committee	Prof. Jaesung Hong	(인)
Committee Member	Prof. Jeon Il Moon	(인)
Committee Member	Prof. Pyunghun Chang	(인)

MS/RT
201122002

박 재 영. Park, Jaeyeong. Improvement of Target Registration Accuracy with Anatomical Landmarks. Department of Robotics Engineering. 2012. 48p. Advisor Prof. Jaesung Hong, Co-Advisor Prof. Jeon Il Moon.

ABSTRACT

In point-based registration between the patient and the image, skin-affixed markers are attached to the patient's skin. Although registration accuracy is relatively high in the region around the markers. The accuracy decreases at a deeply seated target in the body, in proportion to the distance from the surface where the markers are attached. To decrease target registration error (TRE) around the target rather than fiducial registration error (FRE) around the skin markers, additional points should be considered for the registration near the target organ. In this study, a method is proposed that uses an anatomical landmark around the target as an additional point for the registration to decrease TRE.

Keywords: registration, ultrasound, surgical navigation

Contents

List of Tables

List of Figures

Ⅰ. INTRODUCTION

1.1 Surgical Navigation Accuracy

Surgical navigation systems are being increasingly used in a variety of surgery fields, such as cranial nerve, head and neck, ear-nose-and-throat, and orthopedic surgery[1-5]. The main purpose of surgical navigation is to make surgeries safer and more accurate[6]. These navigation systems guide surgical instruments by using medical images. By using a pre- and intra- operative medical image as a map for guidance, surgeons can easily recognize invisible tumors concealed by organs [7]. Compared with conventional surgery, surgical navigation systems allow linking the preoperative three-dimensional image to the patient in the operating room. By projection onto the preoperative image, surgical tools also can be tracked in real time [8]. In conventional surgery, surgeons depend on preoperative medical images and their intuition, both of which have low reliability. However, as surgical navigation provides information in real-time during surgery, surgeons can operate more accurately and without having to use their intuition.

Successful surgical navigation depends on accurate registration between the medical image and the patient [9]. If the accuracy of patient-image registration can be improved, the navigation system will be more successful. In this regard, a method which can improve the registration accuracy between the patient and the image will be proposed and evaluated in this study.

Three kinds of registration protocols are generally used for patient-image registration: point based [10, 11], surface matching [12, 13], and dental splint registration [7, 14]. Point based registration using skin-affixed markers is the most commonly used method because the markers are non-invasive and easily identified in the patient and image [10]. Point based registration is also reported to be more accurate than surface matching by iterative closest point (ICP) and the dental splint method [15]. The skin affixed markers can only be attached to the patient's skin, and the registration accuracy is relatively high at the region around the markers [7, 15]. The accuracy will gradually decrease proportionally with respect to the distance from the surface where the markers are attached [16, 17]. Since the targets for surgery are commonly located deeply in the patient's body, improved accuracy is required for regions far from the skin.

Fiducial Registration Error (FRE), which is the distance between corresponding fiducial points after registration, is defined to compute and report the amount of error in the performed registrations [18]. FRE is automatically calculated by the navigation system and shown as the mean deviation after registration [19]. The error at the target is referred to as Target Registration Error (TRE), which is the distance between a pair of corresponding points not used in the registration process [18]. In TRE terminology, "target" is used to suggest that the points are directly associated with the registration. In medical applications, they are typically points within, or on the boundary of lesions to be excised during surgery or regions of functional activity to be examined for diagnostic purposes. Unfortunately, since the actual target location is unknown during surgery, errors in the clinical target regis-

tration cannot be measured by the registration system. Thus, intentionally or unintentionally, FRE is always regarded as TRE in the medical community [16].

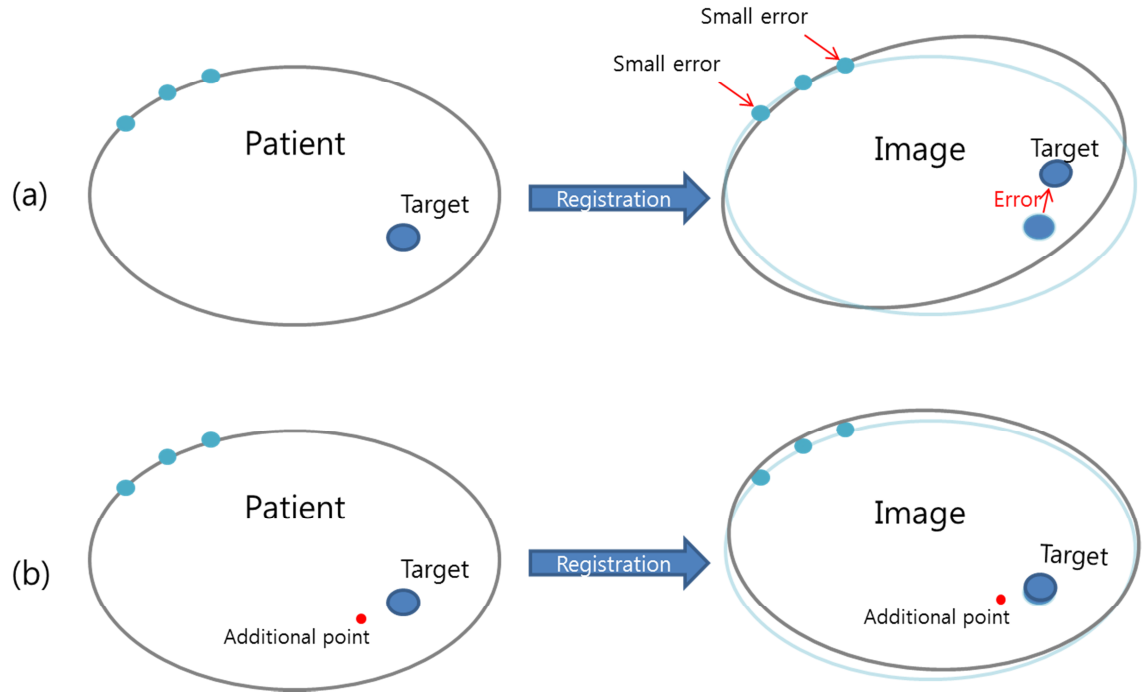

Figure 1.1 Relationship between FRE and TRE; (a) Relatively small FRE and large TRE; (b) Relatively large FRE and small TRE

However, FRE cannot guarantee the accuracy of target registration. Figure 1.1 shows the relationships between FRE and TRE. As shown in Figure 1.1 (a), even with a small error near the fiducial makers TRE can gradually increase proportionally respect to the distance from the surface where the markers are attached. To decrease TRE rather than FRE, additional points that are located within the body or organs are required. Figure 1.1 (b) shows that a relatively small TRE occurs when

additional points near the target area inside the patient are included. Thus, if the additional point can be included into the marker set, better target registration accuracy is expected.

Since ultrasonography is a real-time non-invasive imaging method which is relatively cheaper than other medical imaging systems, it is commonly used to examine inside of a patient's body [20]. Accordingly, this study uses ultrasonography to find anatomical landmarks as additional points and uses these points as fiducial markers for patient-image registration.

1.2 Related Research

Surgical navigation systems are common and commercially available. The StealthStation (Medtronics, Inc., MN, US) and VectorVision (BrainLab, Inc., NJ, US) are widely used commercialized systems (Morioka et al. 1999; Gumprecht, Widenka, and Lumenta 1999). The accuracy of these surgical navigation systems depends on accurate registration. The goal of registration is to find a geometric transformation that aligns points in one image to corresponding points in another image [11]. Numerous studies have been performed to improve the accuracy and convenience of the registration [16, 19]. Hong developed an efficient point-based registration program which can improve the accuracy of the registration [19]. Wenbin demonstrated that effective fiducial configuration decreases TRE [16]. Better accuracy can be expected as a result of this research to improve registration accuracy. However, the fundamental problem, which is that the TRE can gradually increase proportionally with respect to the distance from the surface, still exists. The properties of TRE have been under investigation during the past several years. West demonstrated that improvement in fiducial heuristics decreased the TRE rate in neurosurgery [10]. Fitzpatrick derived an approximation of the root mean squared value of TRE and gave an equation for calculation of expected TRE [17]. According to these studies of TRE, the best configuration of skin-affixed markers is location of the markers near the target position.

Recently, intraoperative medical images have been used in surgical navigation such as X-ray fluoroscopy, ultrasound, and magnetic resonance (MR). Since ultrasound images can be acquired at relatively high speed and low cost, many navigation systems based on an ultrasound diagnostic system have been reported. These reports show that surgical navigation of abdominal organs can be realized effectively [21-24]. A 3D ultrasound-based navigation system has been used to guide radiofrequency thermal ablation (RFA) of liver malignancies [21]. A surgical navigation system guided by intraoperative 3D ultrasound images acquired with an ultrasonic probe placed in contact with the liver has been used effectively in an open abdominal surgery involving hepatectomy [22]. A surgical navigation system guided by an optical and magnetic tracking system shows an overlay of a calculated three-dimensional model of a liver bevacizumab (BV) in an endoscopic image, in which the three-dimensional model is calculated by using two-dimensional ultrasound images acquired from an ultrasound probe placed in contact with the liver under a laparoscope [23, 24]. The advantage of these navigation systems is real-time navigation using ultrasound. Thus, it is possible to navigate deformable abdominal organs. However, ultrasound cannot be used in head and neck surgery because the skull bone fully reflects the ultrasound beam. The ultrasound image has relatively low accuracy and is more difficult to read than other preoperative medical images.

To address these issues, I suggest a method which can include anatomical landmarks as additional fiducial points using an ultrasound system. Since the suggested method using anatomical

landmarks as additional fiducial points, the problem which is error increase proportionally to the distance from the surface can be solved. Thus, better accuracy near the target region is expected.

1.3 Aim of the Study

The current study has three main objectives,

1. To increase the accuracy of registration and find a non-invasive method that can include additional fiducial points that are located within the body or organs.

2. To evaluate and analyze the registration accuracy with- and without additional fiducial points detected by ultrasonography.

3. In that ultrasonography has image distortion caused by its own physical properties, to investigate the effects that are caused by ultrasound distortion to patient-image registration.

1.4 Overview

This work was performed to improve the accuracy of patient-image registration by using an ultrasound diagnostic system which can include anatomical landmarks as additional fiducial makers.

In Chapter 2, the specific method of this study will be addressed. System configuration and ultrasound transducer calibration method will be suggested.

In Chapter 3, the effect of ultrasound distortion in the suggested method will be addressed theoretically and experimentally. Since several ultrasound distortions in different media affect the ultrasound image, the ultrasound image may have errors. How much these errors affect the suggested method and how we can overcome this issue will be addressed in this chapter.

In Chapter 4, to evaluate the suggested method, specific methods of experiments will be addressed. Phantoms and a program were developed for the experiment and the error measuring method will be introduced. The conventional point base registration and suggested registration method will be compared.

In Chapter 5, results of experiments on ultrasound distortion and the registrations will be addressed. The difference between conventional methods and the suggested method will be shown, and the amount of ultrasound distortion will be analyzed.

In Chapter 6, the limitations of using ultrasound will be discussed together with suggestions for improving this study. The current issues and future work will also be discussed. Finally, conclusions will be presented in Chapter 7.

Ⅱ. DEEP POINT REGISTRATION

2.1 The Proposed Method

To take an anatomical landmark as an additional fiducial point, an ultrasound system (ACUSON X300, Simens, Germany) and 3D ultrasound probe (C7F2, Simens, Germany) were used. An optical position sensor (Polaris Vicra, NDI, Waterloo, Canada) was utilized track the surgical tool and ultrasound probe. 3D Slicer (Brigham and Women's Hospital, Boston, USA), which is a free, open-source software, was used as a basic platform software in this research. The proposed system consists of 3D Slicer, a tracker client (NDI, Canada), and a registration client [7].

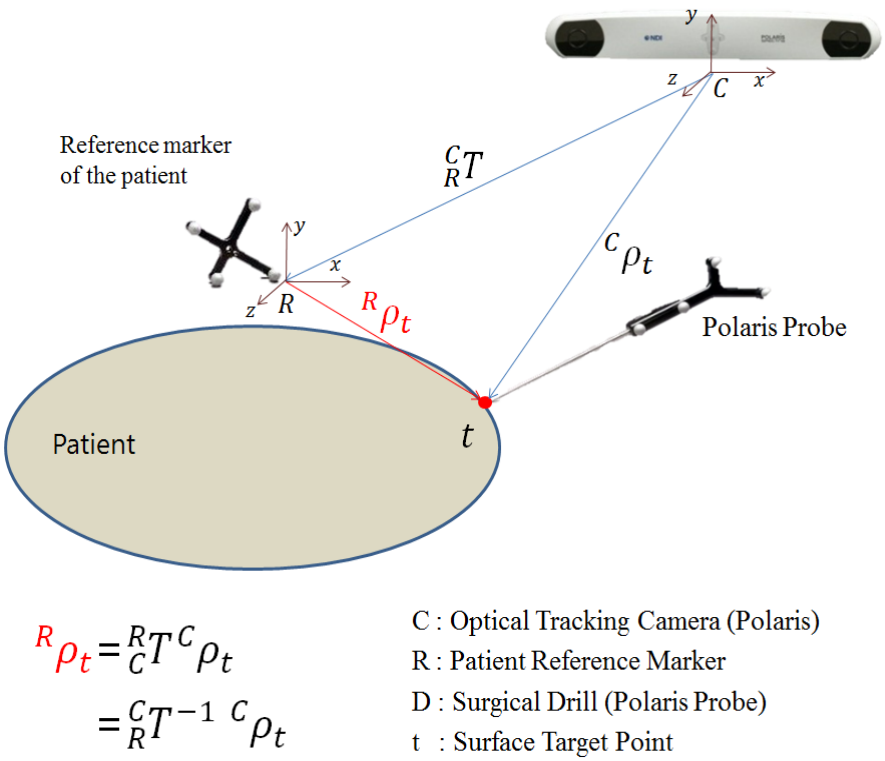

$$^{R}\rho_t = {}^{R}_{C}T\,{}^{C}\rho_t = {}^{C}_{R}T^{-1}\,{}^{C}\rho_t$$

Figure 2.1 Conventional method to acquire position of a fiducial point for patient image registration

Figure 2.1 represents the conventional method to acquire the position of a fiducial point for

the patient-image registration. Optical sensors which are infrared reflectors were attached to the patient reference marker and a probe. The optical tracking system was used to track the position of the probe and the patient reference maker. Two coordinate systems, an optical camera coordinate system represented by a "C" in the figure, and a reference marker coordinate system represented by an "R" in the figure were used. The transformation matrix ${}^{C}_{R}T$ can be calculated by quaternion values which are given by the optical tracking system. The fiducial maker position, with respect to optical camera which represents vector ${}^{C}\rho_t$ was also given by the optical tracking system. Thus, the target position with respect to the reference maker which is represented as vector ${}^{R}\rho_t$ can be calculated as shown in equation 2.1.

$${}^{R}\rho_t = {}^{R}_{C}T \; {}^{C}\rho_t = {}^{C}_{R}T^{-1} \; {}^{C}\rho_t \qquad \text{Equation 2.1}$$

Figure 2.2 represents the suggested method to acquire an additional fiducial point using ultrasonography for patient-image registration. Optical sensors were attached to the ultrasound probe, and the optical tracking system was used to track the position of the probe. Additional fiducial points were taken from the ultrasound images using the optical position sensor that recognizes the position of the ultrasound probe. After appropriate transformations, the reference points were treated as the markers for registration, as with surface markers. Compared to conventional methods, there is one more coordinate system that is ultrasound probe. Thus, there are three coordinate systems which are represented by C, R, and U. C represents the optical tracking camera, R represents the reference marker of the patient, and U represents ultrasound probe coordinate system. Transformation matrices ${}^{C}_{R}T$ and ${}^{C}_{U}T$ can be calculated by quaternion values which are given by the optical tracking system.

The transformation matrix from the patient reference marker to the ultrasound probe is given by ${}^{R}_{U}T$ in the figure and can be calculated as shown in the equation 2.2. If we know the vector ${}^{U}\rho_t$ which is the depth reference target position with respect to the ultrasound coordinate system, the position with respect to patient reference marker ${}^{R}\rho_t$ can be calculated as shown in equation 2.3.

$${}^{R}_{U}T = {}^{C}_{R}T^{-1}\,{}^{C}_{U}T \qquad \text{Equation 2.2}$$

$${}^{R}\rho_t = {}^{R}_{U}T\,{}^{U}\rho_t \qquad \text{Equation 2.3}$$

Since the ultrasound probe and the image acquired from the ultrasound system have different coordinate systems, calibration between the ultrasound probe and the ultrasound image is needed.

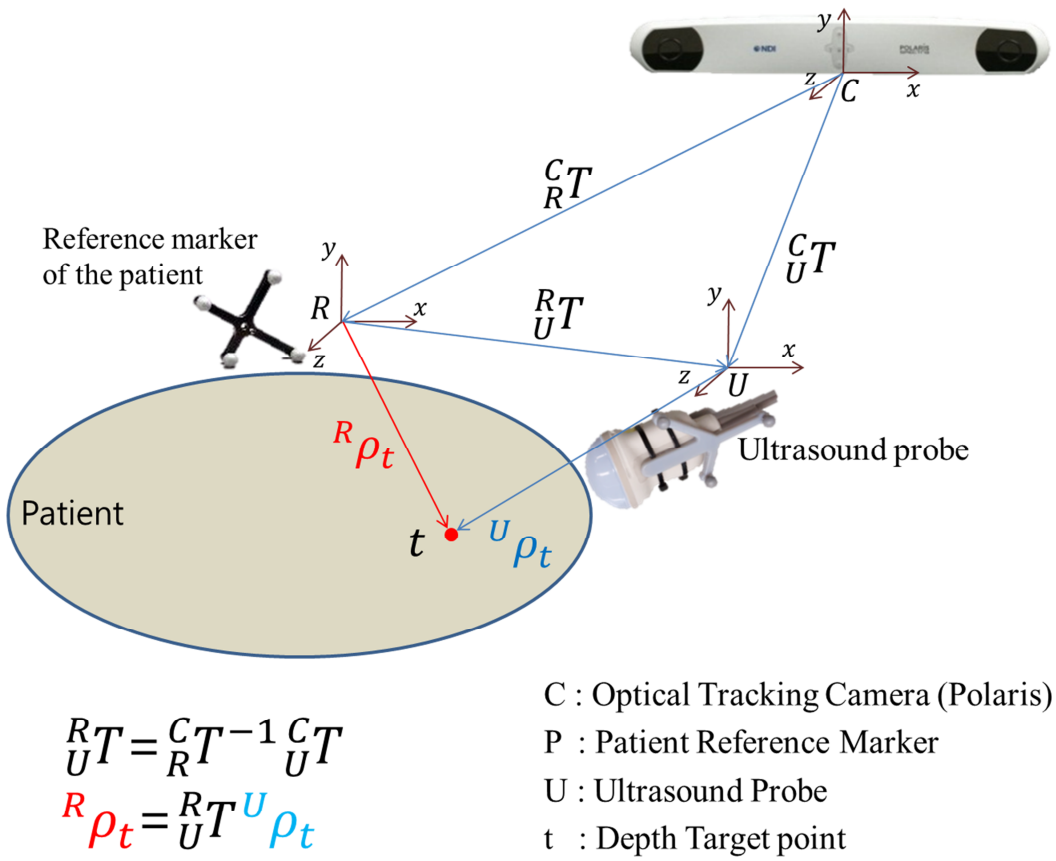

Figure 2.2 Suggested method to acquire fiducial position for patient image registration

2.2 System Configuration

TRE gradually increases proportionally to the distance from the surface where the markers are attached. To decrease TRE rather than FRE, additional points located within the body or organs are required. To take the additional points, an ultrasound probe is used with an optical tracking system. To acquire both the position of fiducial markers attached to the patient's skin and the anatomical landmark position, a surgical probe and an ultrasound probe are used simultaneously.

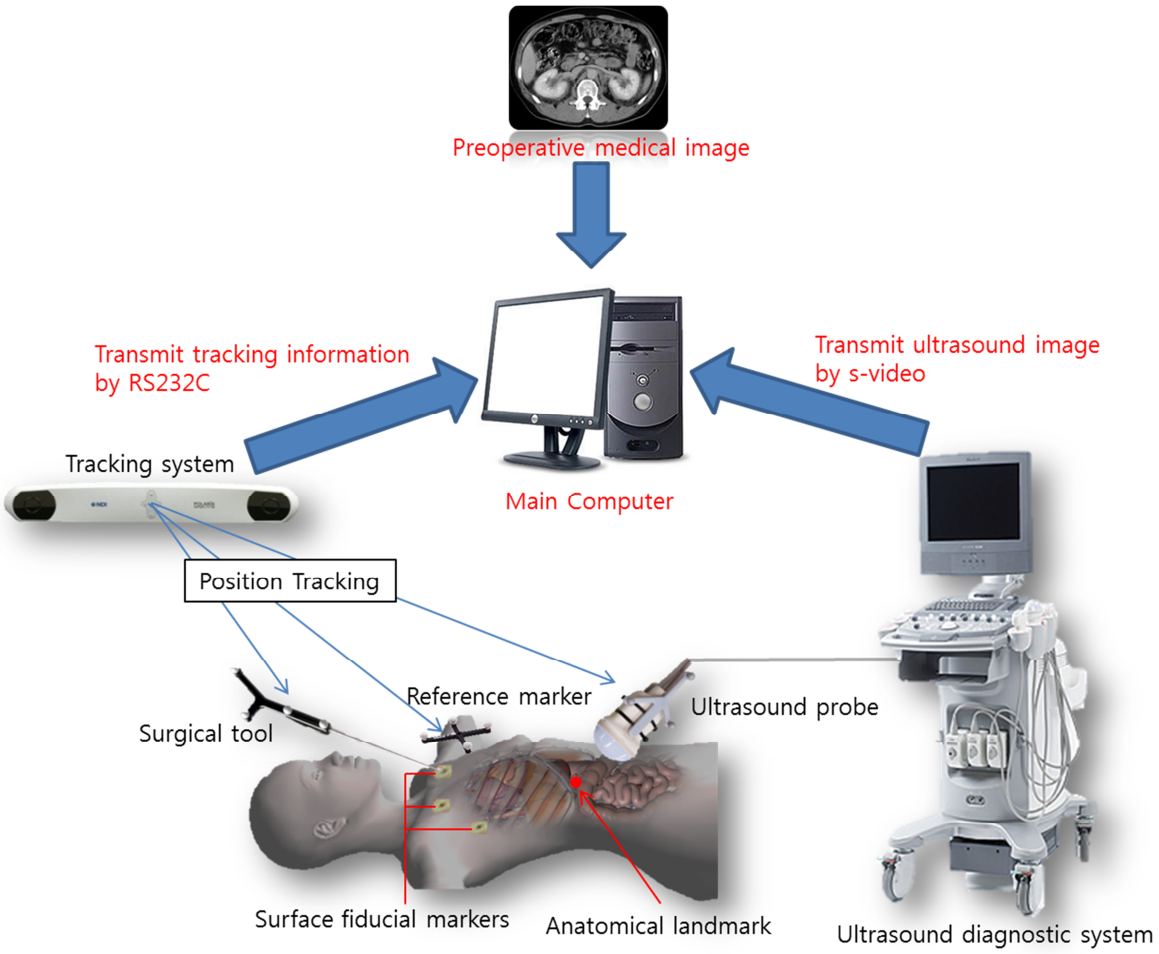

Figure 2.3 System configuration of suggested method

Figure 2.3 shows the whole system configuration for patient-image registration using deep anatomical landmarks. Surface fiducial markers are markers that is attached to the patient skin and identified in the medical images for registration. Reference marker is a set of infrared reflecting markers that are attached to the patient to compensate patient movement. Anatomical landmark is sharp corners or edges of bone, vessel, or any other organs in the body that can play a role as markers for the registration.

The surgical probe acquires positions of skin-affixed fiducial markers and the ultrasound probe acquires an anatomical landmark. To compensate for the patient's movement, a reference marker is attached to the patient's skin. The coordinates of each probe and marks tracked by the tracking system are transmitted to the main computer by RS232C communication. The ultrasound diagnostic system transmits the ultrasound image to the main computer by s-video. Then, the main computer captures the ultrasound image. The additional fiducial points are taken from the ultrasound images in the computer. After appropriate transformations, the additional points can be treated as the markers for the registration like surface fiducial markers. The main computer performs patient-image registration between these fiducial markers including additional points and preoperative medical image such as MR and CT image.

2.3 Ultrasound Transducer Calibration

As shown in Figure 2.4, the ultrasound transducer and the image have different coordinate systems. To know the position of an additional fiducial point with respect to the world coordinate system from the ultrasound image, calibration of the ultrasound transducer is needed. After calibration between the ultrasound transducer and image, the additional point can be treated as a fiducial marker for patient-image registration.

To calibrate between the ultrasound transducer and an image, the relationship between their coordinate systems must be known. The ultrasound transducer can be tracked by an optical tracking system but an ultrasound image cannot be. Thus, a calibration tool is needed to know the position of the ultrasound image that can be tracked by an optical tracking system. That calibration tool requires a minimum of three landmarks to calibrate.

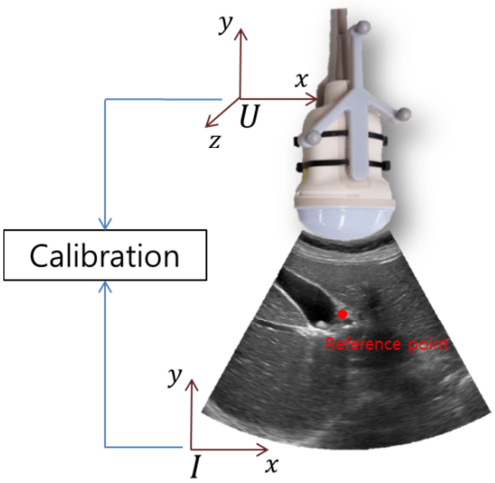

Figure 2.4 Different coordinate system between ultrasound transducer and image

To calibrate the ultrasound transducer, a calibration box (Figure 2.5) that has special landmarks was manufactured using a three dimensional printing system (EDEN250, Objet, Israel). Since an ultrasound image is a two-dimensional coordinate system, the landmarks are arranged in parallel to the ultrasound transducer. To track the calibration box position, optical sensors are attached to the calibration box, as shown in Figure 2.5. Optical sensors were also attached to the ultrasound probe to track the ultrasound probe position, as shown in Figure 2.4. The positions of the landmarks with respect to the optical sensors were given by the geometry of the calibration box. The calibration box was filled with pure water as a medium for ultrasound.

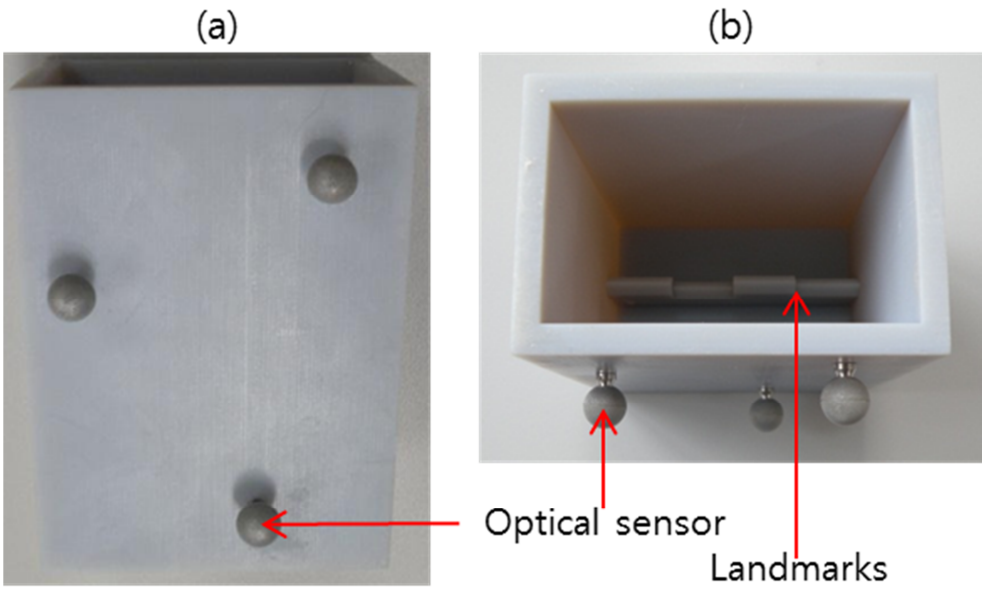

Figure 2.5 Calibration box. (a) Front view; (b) Top view

For calibration between the ultrasound image and the ultrasound probe, the registration client [19] was applied with paired point registration method. This method computes a transformation matrix using at least three paired points between the patient and the image.

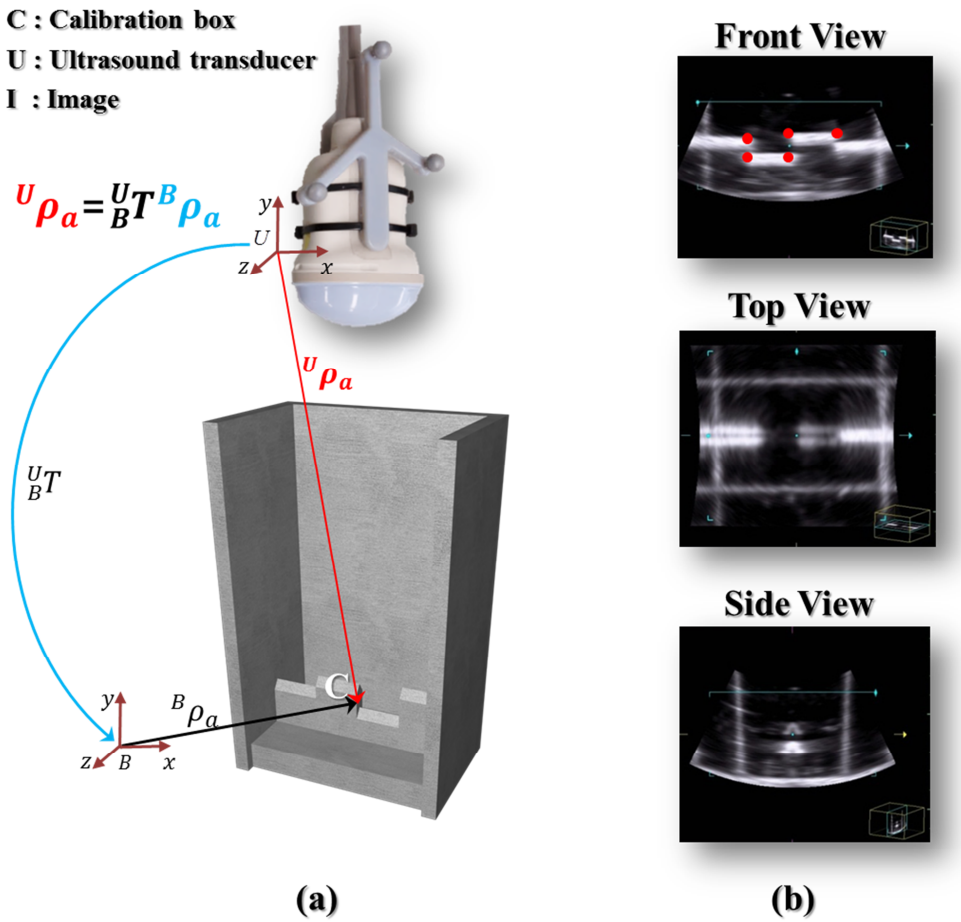

Figure 2.6 Calibration box coordinate systems and its ultrasound images (a) Method to acquire a landmark from the ultrasound probe coordinates to the calibration box coordinates; (b) Ultrasound images of the calibration box.

Five points were selected from the ultrasound image (red dot in figure 2.6 (b)). The points were specified on the images by the manipulation of a computer mouse. In addition, the coordinates of five corresponding points on the calibration box were acquired by the tracking system (Figure 2.6 (a)).

Ⅲ. ULTRASOUND DISTORTION ANALYSIS

3.1 Literature Review

Ultrasonography has been broadly used for over half a century as a medical imaging technique with real-time and non-invasive results. It is an ultrasound-based diagnostic imaging technique for visualizing subcutaneous body structures. Ultrasound applies to all sound waves with a frequency above the audible range (16~20,000 Hz) of normal human hearing. The frequencies used in diagnostic ultrasound are typically between 2 and 18MHz. Fundamentally, the physical property of ultrasound is the same as audible frequency.

The propagation speed of ultrasound through tissue depends on the properties of the tissue, in particular the stiffness (β), the density (ρ) and compressibility (k) [20].

$$c = \sqrt{\frac{\beta}{\rho}} = \frac{\beta}{\sqrt{k\rho}} \ (m/sec)$$

As a general rule, gases have the slowest propagation speed, liquids have an intermediate propagation speed and firm solids have a high propagation speed. Table 3.1 shows the propagation speed and density of different media [25].

Table 3.1 Ultrasound propagation speed and density of medium

Medium	Propagation speed (m/s)	Density (kg/m^3)
Air	330	1.29
Lung	600	300
Fat	1,450	920
Water	1,490	1,000
Soft Tissue	1,540	1,050
Liver	1,555	1,061
Blood	1,560	1,058
Kidney	1,565	1,041
Muscle	1,680	1,068
Acrylic Resin	2,670	1,180
Bone	4,080	1,912

Because of the physical property of ultrasound, ultrasound images have image distortion depending on the medium. Since ultrasonography was used to find the position of anatomical landmarks that were used as fiducial markers for the patient-image registration, the ultrasound image distortion may affect the patient-image registration. In this section, ultrasound distortion will be studied by theoretical and experimental methods, and the amount of impact ultrasound distortion has on image registration will be discovered.

The kinds of ultrasound distortion are reflection, refraction, scattering, and slicer thickness resolution. Reflection can cause mirror images, but usually these mirror images can be distinguished by the user. Since the objective of ultrasound is larger than the wavelength of ultrasound, scattering also can be ignored. However, diffused reflection which is also called scattering can occur near the surface of the objective. This diffused reflection can make image blur and this image blur makes it

difficult to choose pointing out the additional point precisely.

Refraction also occurs at the surface where the between two different medium. Refraction is the change in direction of a wave due to a change in its medium. Because of ultrasound refraction, the ultrasound image may have image distortion. Since anatomical landmarks are located in the human body, this image distortion caused by ultrasound refraction could affect the suggested method. In Section 3.3, the refraction error in the ultrasound image will be studied.

Ideally, an ultrasound image is two-dimensional as if cut by a razor. However, since ultrasound transducers have their own thickness and wavelength of ultrasound, an ultrasound image may include thickness information perpendicularly to the direction of the ultrasound beam. In Section 3.4, errors which can be caused by this thickness will be studied.

3.2 Diffused Reflection

At the boundary between two different types of tissue, an ultrasound wave is partially reflected and partially transmitted. The relative proportions of the energy reflected and transmitted depend on the acoustic impedance (z) of the two materials [20]. The acoustic impedance of a material is governed by its density (ρ) and stiffness (k) such that

$$\mathrm{z} = \sqrt{\rho \cdot k}$$

The amplitude of the reflected wave is proportional to the difference in the acoustic impedance of the two materials. For perpendicular incidence of the ultrasound beam on a large flat interface the amplitude reflection coefficient (R) is given by

$$\mathrm{R} = \frac{Z_2 - Z_1}{Z_2 + Z_1}$$

Where Z_1 and Z_2 are the acoustic impedances of the first and second tissues respectively.

Diffused reflection, which is called scattering, occurs at rough the boundary between two different types of tissue. In the ultrasound image, image blur can occur at the region near the boundary of tissues by diffused reflection. Figure 3.1 shows diffused reflection and image blur in an ultrasound image.

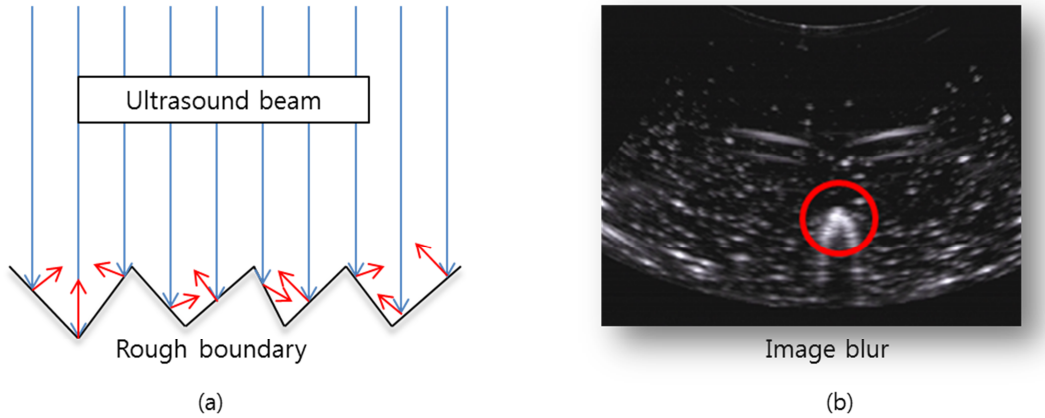

Figure 3.1 The diffused reflection of an ultrasound beam and image blur (a) Diffused reflection at the rough boundary (b) Image blur caused by diffused reflection

Since anatomical landmarks in the human body are usually the edge point of bone or organs, diffused reflection occurs at that region. Degrees of diffused reflection are based upon acoustic impedance, roughness of medium, and frequency of ultrasound.

Image blur can occur by scattering and reflection on the surface of tissue. Since the position of anatomical landmarks is selected by computer mouse, image blur could make localization errors when the user points out the position of the anatomical landmark on the ultrasound image. The degree of image blur could be different depending on the roughness and quality of the medium, but the landmark location cannot be detected precisely because of image blur. To discover the error affected by these localization errors, a phantom experiment was performed.

3.3 Refraction

The refraction angle of ultrasound depends on the velocity of sound in the medium and incidence angle, in particular the refraction angle (θ_t), the incidence angle (θ_i), velocity of sound in incidence plane (C_1) and the velocity of sound in refraction plane (C_2) [20]. When the propagation speed of medium 1 is faster than that of medium 2', the refraction angle is larger than the incident angle.

$$\sin\theta_t = \frac{C_2}{C_1} \times \sin\theta_i$$

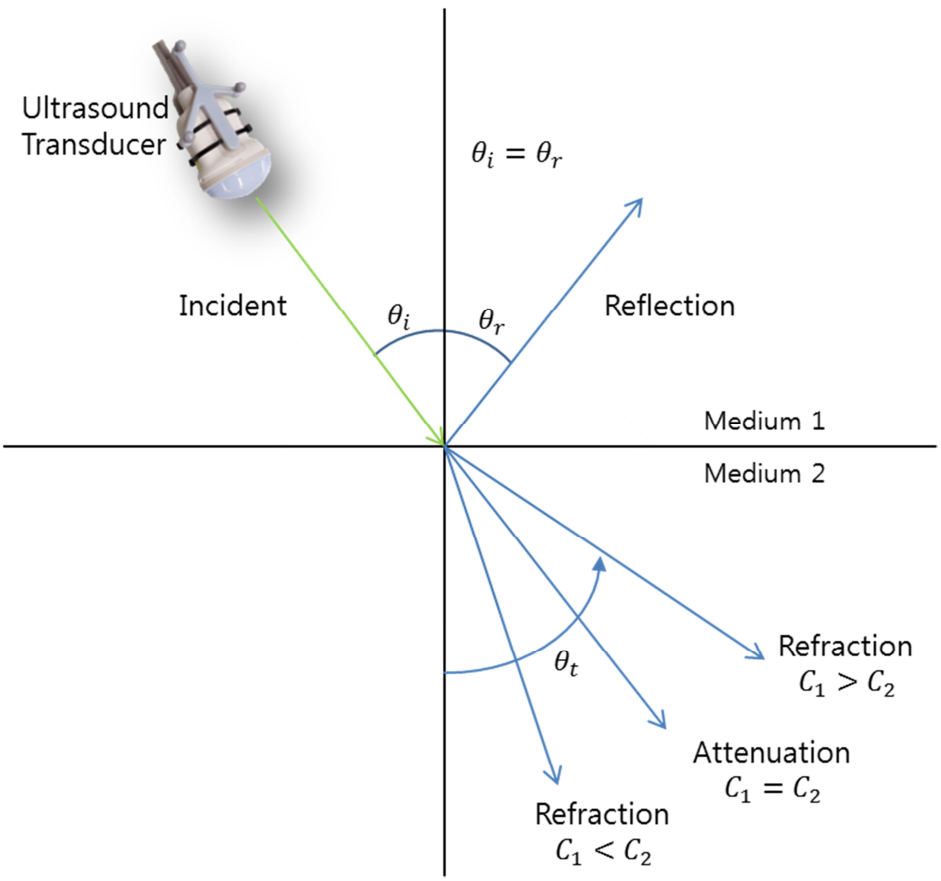

Figure 3.3 Refraction of ultrasound

Since anatomical landmarks are located in organs or bone inside the human body, they

might be surrounded by fat, muscle and blood. Since fat, muscle and blood have different propagation speeds, refraction can occur when using ultrasound diagnosis systems in a real human body. Therefore, refraction errors cannot be ignored when using ultrasound diagnosis systems.

3.4 Beam Thickness

The thickness of an ultrasound beam is perpendicular to the image of ultrasound. The beam thickness is one of image resolution and depends on the size of piezoelectric material in transducer. The frequency of ultrasound and focal length also affect the beam thickness.

The ultrasound image is reconstructed by stereoscopic ultrasound beam, and the thickness of the beam is thinnest at the focal depth. From there, the beam gets proportionally thicker the farther one moves from the focal depth.

Because of beam thickness, errors which are in perpendicular in direction to the ultrasound image could occur when the position of anatomical landmarks were found using the suggested method. The amount of the error will be different based upon the transducer size, frequency, focal length, and users.

Ⅳ. Experiments

4.1 Phantom Preparation

Registration Experiments Phantom

To evaluate the proposed method, a special-purpose phantom was manufactured using a three dimensional printing system. The phantom was a 83 × 85 × 83 mm hexahedron. The material of the phantom is acrylic resin which has a similar propagation speed to bone. Skin-affixed markers were attached on the outer surface and used as skin fiducial markers during registration. Since anatomical landmarks could be the edges of a bone in a real human case, cone-shaped landmarks were made inside the phantom to mimic the real environment. The cone-shaped landmarks were easily detected by the ultrasound system (Figure 4.1).

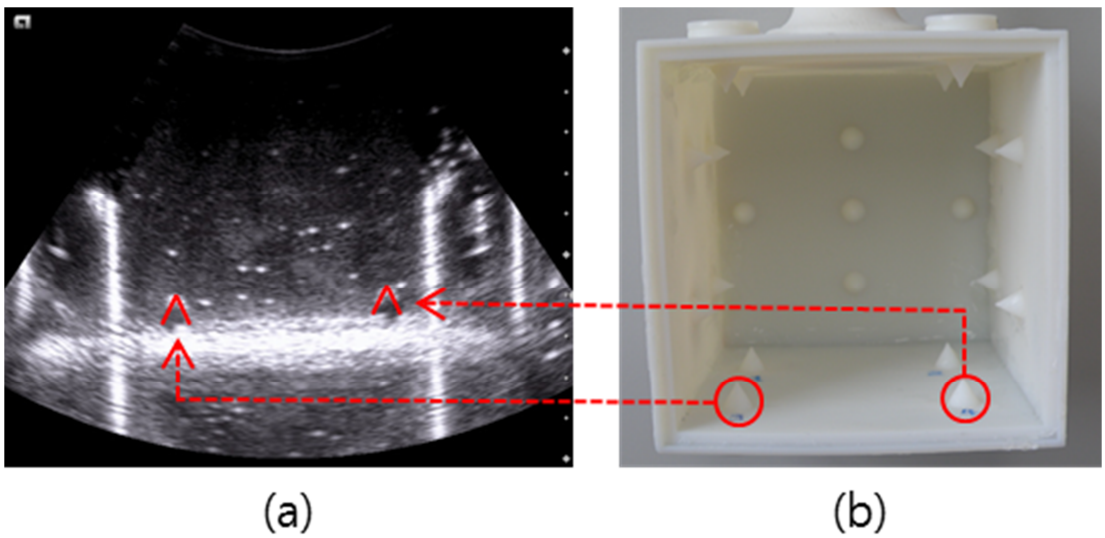

Figure 4.1 Cone-shaped landmarks inside the phantom (a) Ultrasound image of the phantom; (b) Internal view of the phantom.

One-side of the phantom was opened to allow use of an ultrasound probe in water. Optical tracking sensors were attached on the phantom to track position. CT images with 0.6 mm slices were acquired for the phantom (image dimensions 512 × 512 × 172 pixels, resolution 0.2656 × 0.2656 × 0.6 mm).

Diffused Reflection Experiments Phantom

To evaluate the degree to which image blur affects accuracy when technicians select the landmark location, bone and fat phantoms were prepared. The bone phantom was made by a three dimensional printing system and the fat phantom was made using porcine fat. The bone phantom material was acrylic resin as it is relatively similar in propagation velocity and density to actual human bone (Table 3.1). Figure 4.2 shows the bone and fat phantom. To distinguish one point in the image, each phantom has an edge point.

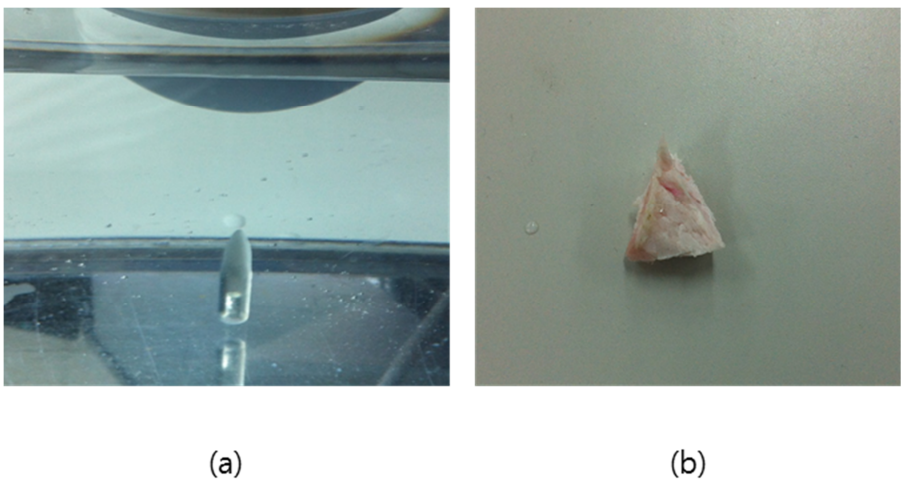

Figure 4.2 Prepared phantoms for diffused reflection experiment; (a) Bone phantom (b) Fat phantom

Refraction Experiments Phantom

To measure the effect of ultrasound refraction when using the suggested method on an actual human body, porcine fat and muscle were prepared for experiments. Figure 4.3 (a) shows a prepared 5.66 mm thickness of fat tissue and (b) 7.18 mm thickness of muscle tissue for the experiments. Each phantom was cut to a 100 × 100 mm size and affixed to a plastic stick.

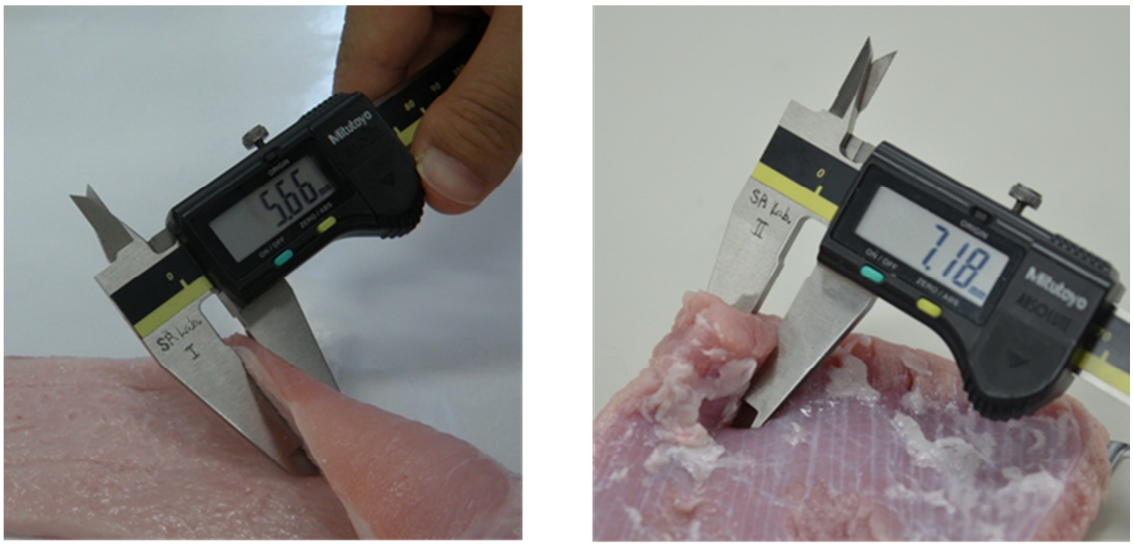

(a) (b)

Figure 4.3 Prepared phantom for refraction experiments (a) Porcine fat (b) Porcine muscle

An acrylic box full of pure water with a similar propagation speed to blood was used for the experiments (Figure 4.4). An ultrasound probe was fixed on top of the water tank. A grid-shaped phantom was soaked in the water to measure the movement of image caused by refraction. Measurement software in the ultrasound system which has an accuracy of 0.1 mm was used for the experiments.

Figure 4.4 Acrylic box filled with pure water. An ultrasound probe was affixed to the top and a grid-shaped phantom was immersed in the water.

Beam Thickness Experiments Phantom

To measure the amount of error caused by ultrasound beam thickness, a thin acrylic phantom was made. The phantom was made from a 1 mm thick acrylic panel. The phantom's dimensions are 40 × 50 × 1 mm. Since the beam thickness direction is perpendicular to the image, the phantom was aligned with the ultrasound transducer. Figure 4.5 shows the thin phantom.

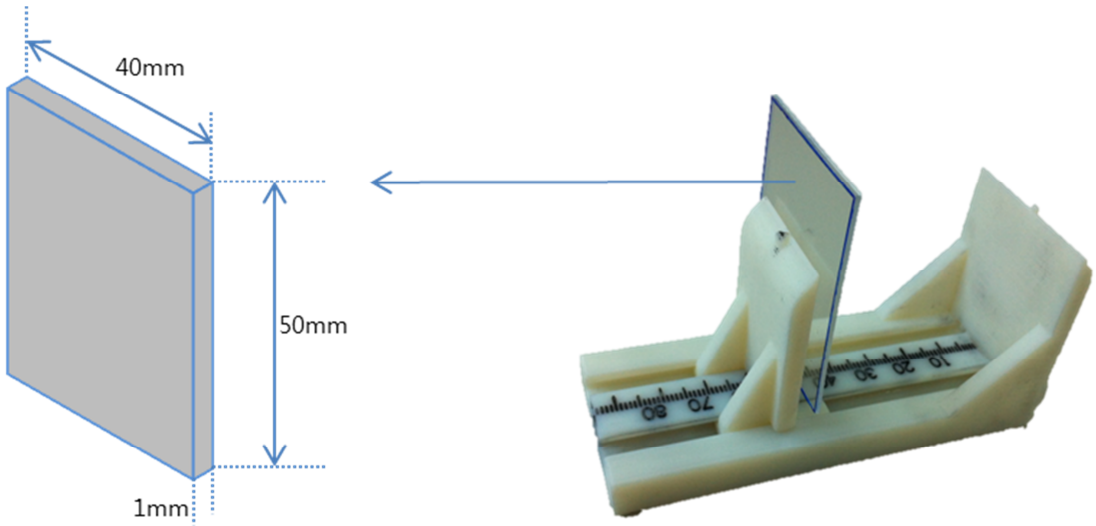

Figure 4.5 The phantom for beam thickness experiments

4.2 Registration Experiments

3D Slicer (Brigham and Women's Hospital, Boston, USA) which is a free open-source software was used as the basic platform software in this research. The proposed system consists of 3D Slicer, a tracking client, and a registration client [7]. To detect and track the surgical probes an optical position sensor (Polaris Vicra, NDI, Waterloo, Canada) was employed.

To evaluate the improvement in accuracy of the proposed method, a phantom experiment was conducted. An acrylic box filled with pure water was used with the ultrasound system. The tracking system tracked both the phantom and the ultrasound probe simultaneously (Figure 4.6). The ultrasound probe detected landmarks (Figure 4.1) inside the phantom. After appropriate transformations, which were calculated during calibration, landmarks can be treated as fiducial markers. The paired point registration method was performed between a reconstructed image of the computed tomography (CT) volume data and the phantom.

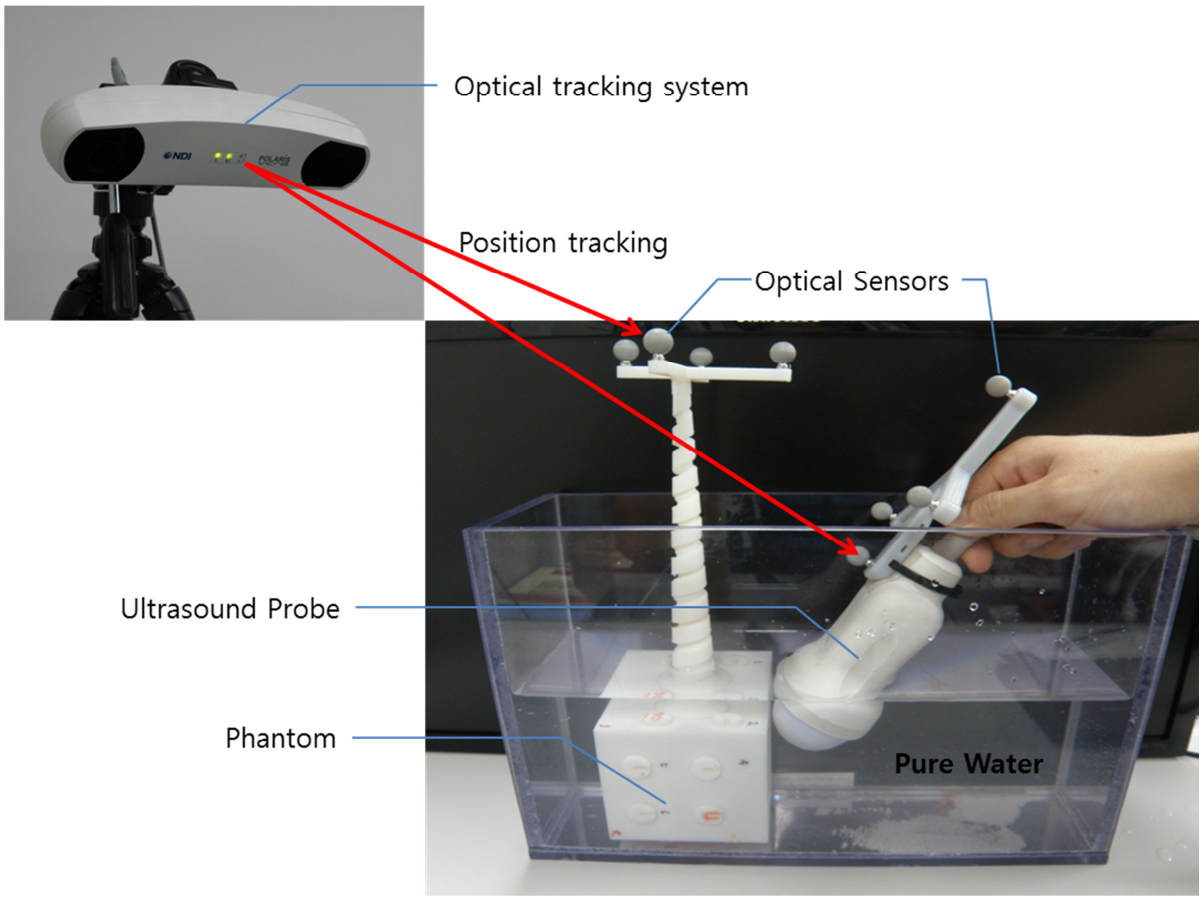

Figure 4.6 Experiment configuration for registration experiment.

Three experiments were performed. First, without an additional fiducial point, six fiducial makers attached to the surface of the phantom were used for registration. Second, with an additional anatomical point, five fiducial markers attached to the surface of the phantom were used for registration. In the second configuration a Polaris probe was used to determine the position of the five fiducial markers, the position of the additional anatomical point was determined by ultrasonography. The third configuration of the experiment was the same as the second, but used a Polaris probe to determine

the position of both the five fiducial markers and an additional fiducial position. FRE and TRE were measured in every experiment. TREs were measured using three of the inner landmarks, excluding the point that was used for the additional anatomical position.

4.3 Ultrasound Distortion Experiments

Diffused Reflection

Ultrasound images of the fat and bone phantoms were taken. Since diffused reflection is affected by material property on the surface and ultrasound frequency, ultrasound images of both the fat and bone phantom were taken at different frequencies. Two multi-frequency ultrasound probes (C7F2 and EV9-4, Simens, Germany) were used. Figure 4.7 shows the ultrasound images of the fat and bone phantom at each frequency.

To find the localization error caused by ultrasound image blur, thirty randomly-selected people were chosen to act as ultrasound technicians for the experiment. Each technician selected the edge of the landmark 10 times using a computer mouse, and the coordinates of each experiment were recorded. Since the actual landmark location was unknown, the localization error was estimated by averaging the measured distances between repeated selections of the same landmarks.

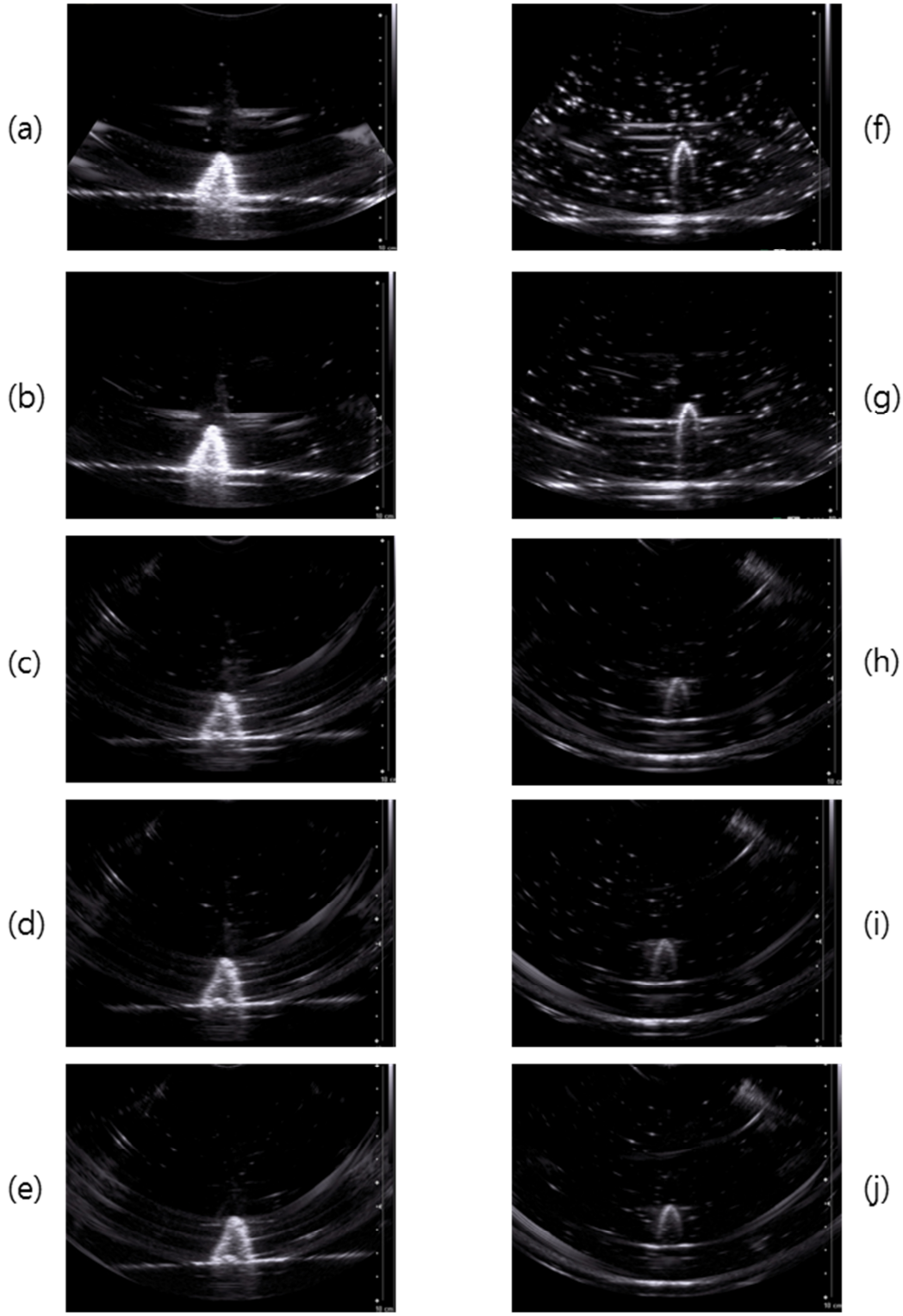

Figure 4.7 Ultrasound image of the fat and bone phantom with different frequencies (a) Fat 2MHz (b) Fat 2.5MHz (c) Fat 5MHz (d) Fat 6.7MHz (e) Fat 8MHz (f) Bone 2MHz (g) Bone 2.5MHz (h) Bone 5MHz (i) Bone 6.7MHz (j) Bone 8MHz

Refraction

Since the material property and the incident angle of the ultrasound beam affect refraction, experiments were set up as shown Figure 4.8 to examine the amount of refraction in different tissues and at different incident angle. Prepared fat and muscle phantoms were used for the experiment. The change in the ultrasound image was measured at incident angles of 15°, 30°, and 45°.

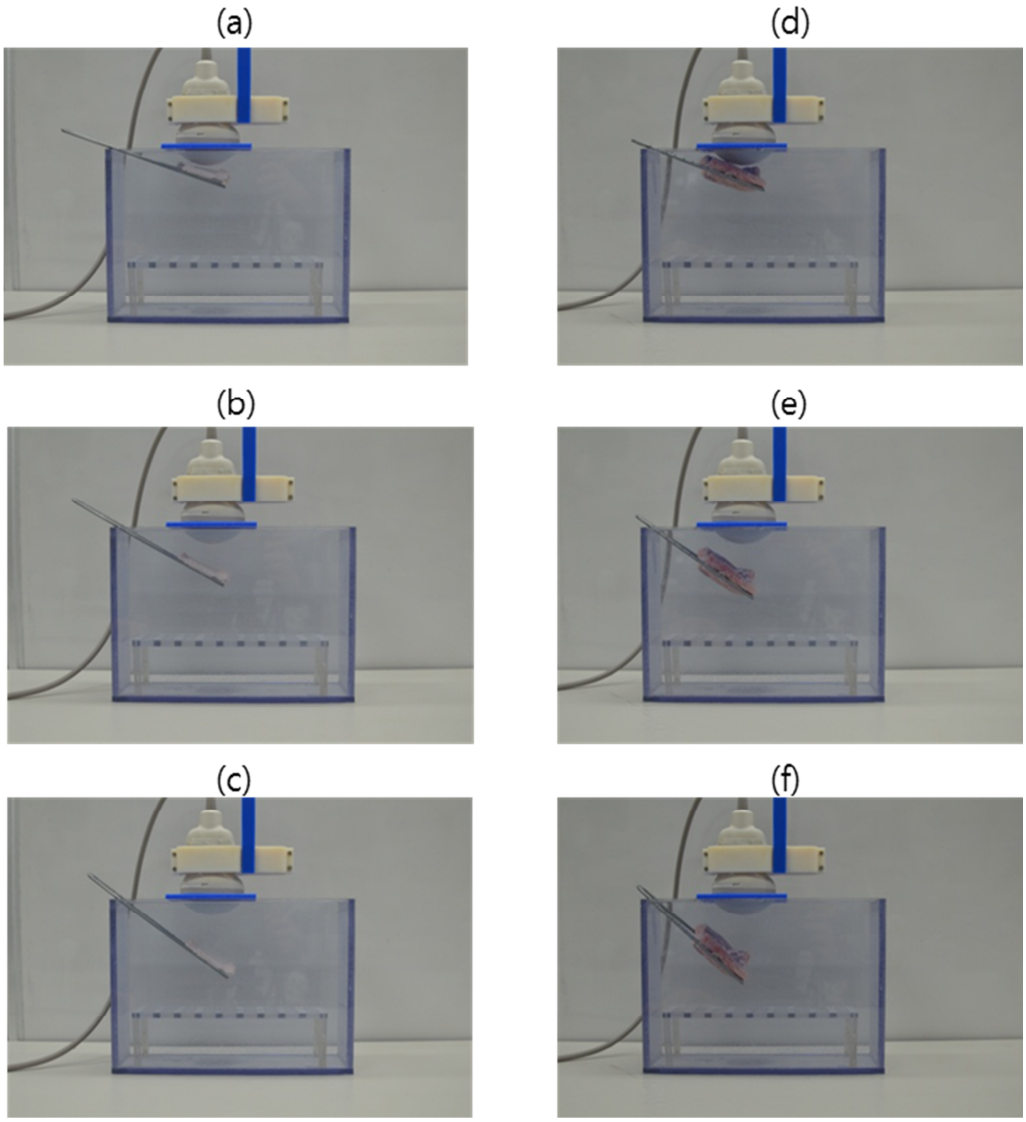

Figure 4.8 Experiment setup for examining ultrasound refraction (a) Fat **15°** (b) Fat 30° (c) Fat 4**5°** (d) Muscle **15°** (e) Muscle 30° (f) Muscle **45°**

Beam Thickness

Beam thickness is dependent on the size of the transducer, focal length, and frequency. The localization error caused by beam thickness is expected to be different among different technicians. In this experiment, the condition of focal length, frequency, and the transducer was the same as in the registration experiment. Thirty people were randomly selected to act as technicians in the experiment. Each technician tried to find the phantom position by moving the ultrasound probe. The phantom position in the ultrasound image of each experiment was recorded.

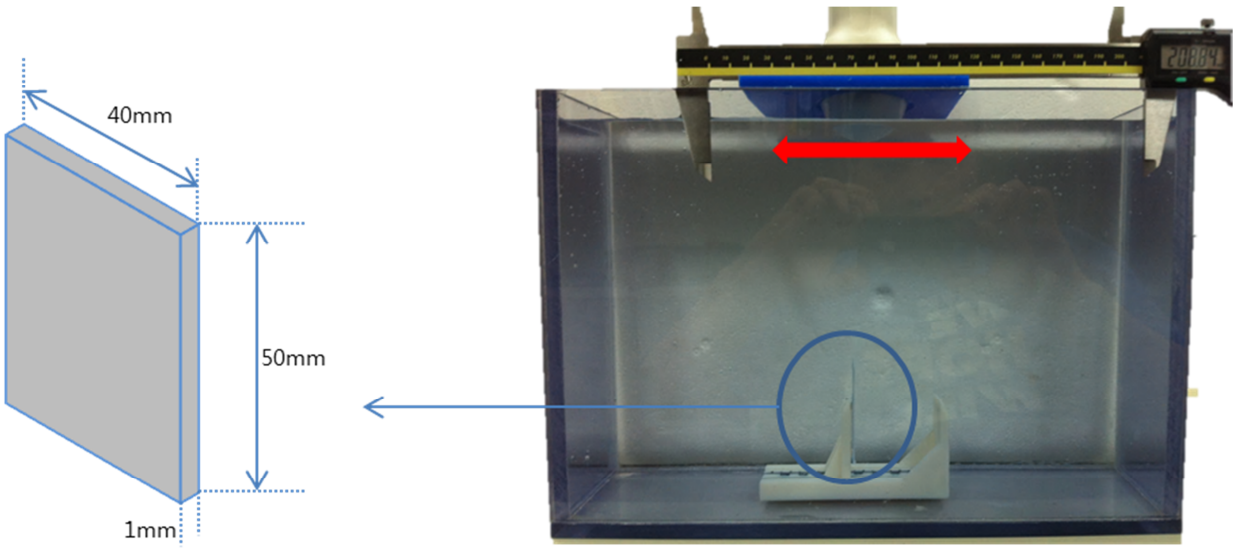

Figure 4.9 Beam thickness experiment setup. An acrylic box filled with pure water was used. The ultrasound probe was affixed on the top of the acrylic box. The thin phantom was algined with the ultrasound probe.

An acrylic box filled with pure water was used for the experiment. The ultrasound probe was affixed on the top of the acrylic box. The ultrasound probe could be moved along the horizontal axis of the acrylic box. The phantom was affixed in the water and it was aligned with the direction of the ultrasound probe. A vernier caliper was attached on the top of the acrylic box to measure the movement of the ultrasound probe.

Ⅴ. Results

5.1 Registration

The registration accuracy with and without an additional fiducial point was examined. Figure 5.1 shows the TREs and FREs of the target fiducial markers. The y-axis represents the scale error in millimeters. Experimental FREs that were determined with and without deep reference points were 1.08 ± 0.29 mm and 1.32 ± 0.18 mm, respectively. Further, average experimental TREs that were determined with and without an additional fiducial point were 1.77 ± 0.352 mm and 1.54 ± 0.233 mm, respectively. It is clear that the use of additional fiducial points caused a slight decrease in FRE and a slight increase in TRE.

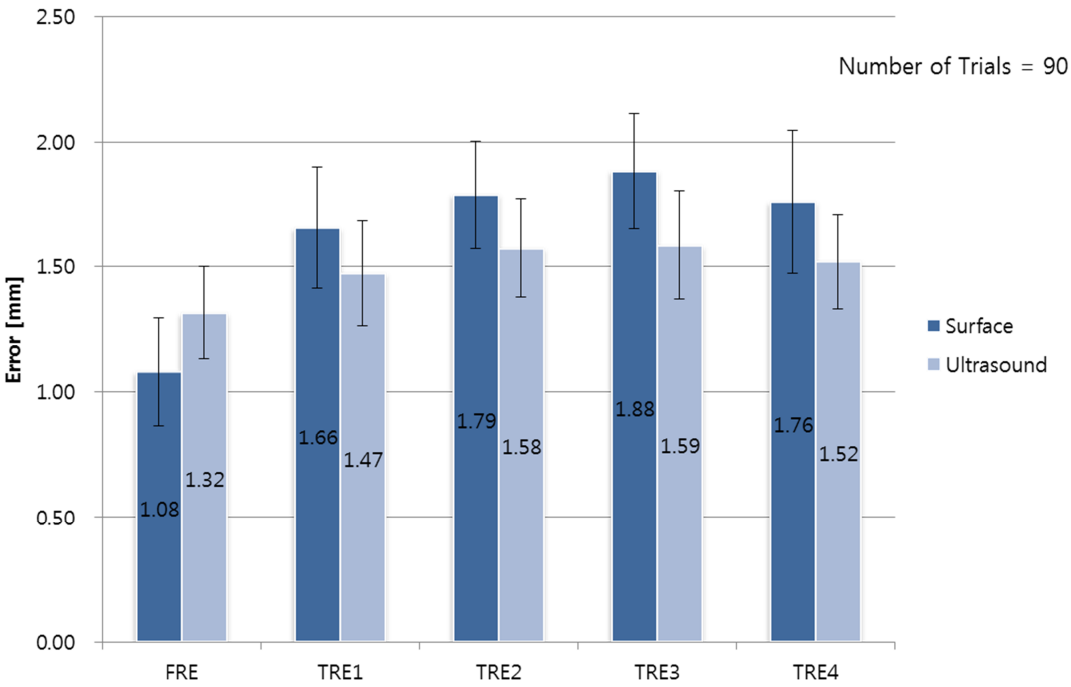

Figure 5.1 Accuracy registration with and without deep reference points.

To evaluate the ultrasound accuracy, I compared the experiments with an ultrasound probe

and a Polaris probe. Figure 5.2 shows the TREs and FREs of the target fiducial markers. The y-axis represents the scale error in millimeters. The experimental FREs determined by the Polaris probe and the ultrasound probe were 1.29 ± 0.29 mm and 1.32 ± 0.18 mm, respectively. Further, average experimental TREs that were determined with and without additional fiducial points were 1.33 ± 0.352 mm and 1.54 ± 0.233 mm, respectively. These results show that the Ploaris probe is slightly more accurate than the ultrasound probe.

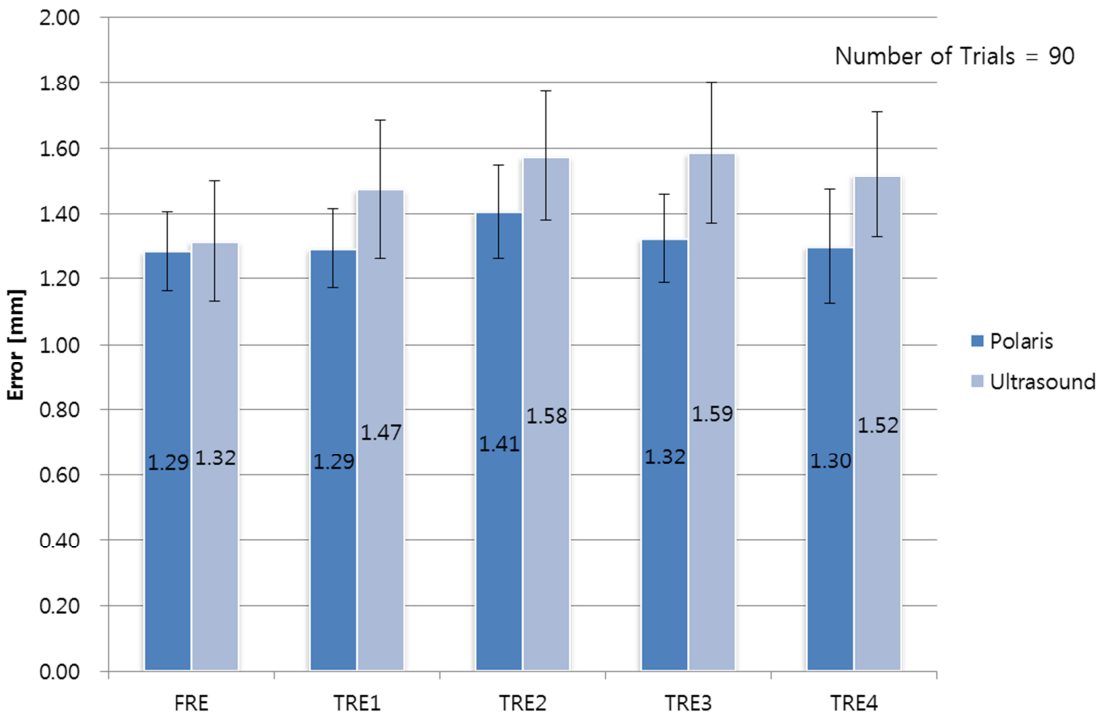

Figure 5.2 Comparison of ultrasound probe and the Polaris probe

5.2 Ultrasound Distortion

Diffused Reflection

I examined the localization error caused by diffused reflection of the fat and bone phantom. Figure 5.3 shows the experiment localization errors. The y-axis represents the scale error in millimeters. Average experimental localization errors of the fat and bone phantom were 0.38 ± 0.10 mm and 0.32 ± 0.08 mm, respectively. It seems difficult to find a relationship between the error and frequencies. The results show that bone phantoms result in slightly smaller errors than fat phantoms.

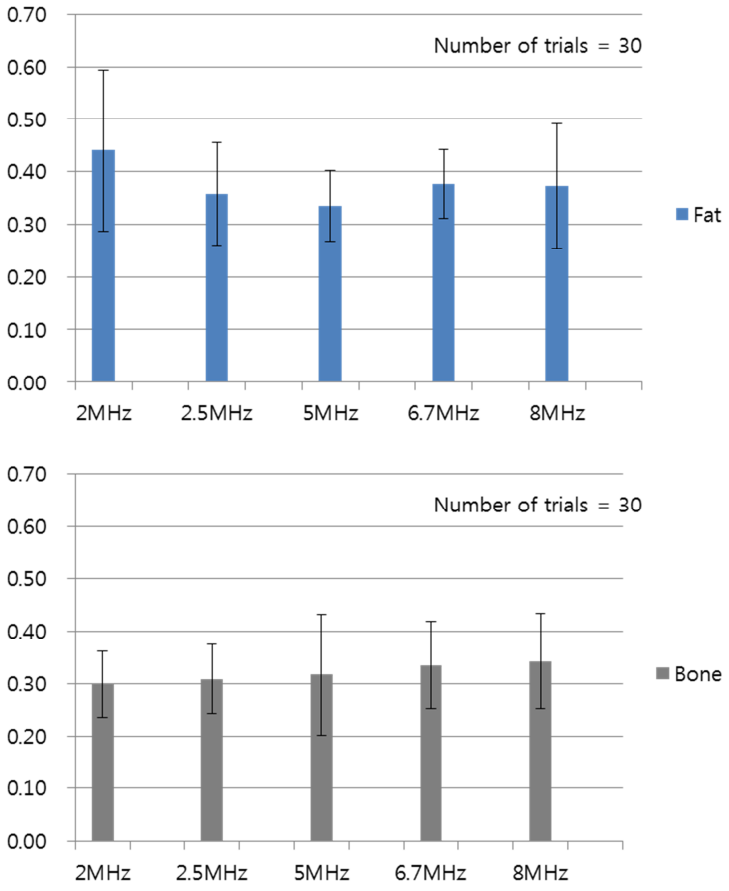

Figure 5.3 Results of diffused reflection experiments, fat and bone phantoms were examined at different frequencies.

Refraction

I examined the error caused by refraction of fat and muscle phantoms at each different incident angle. Figure 5.4 shows the resulting ultrasound images. Table 5.1 shows the refraction errors of fat and muscle phantoms at each incident angle. There is no apparent relationship between the error and frequencies. As with the diffused refraction, the results show that fat phantoms result in slightly smaller errors than fat phantoms.

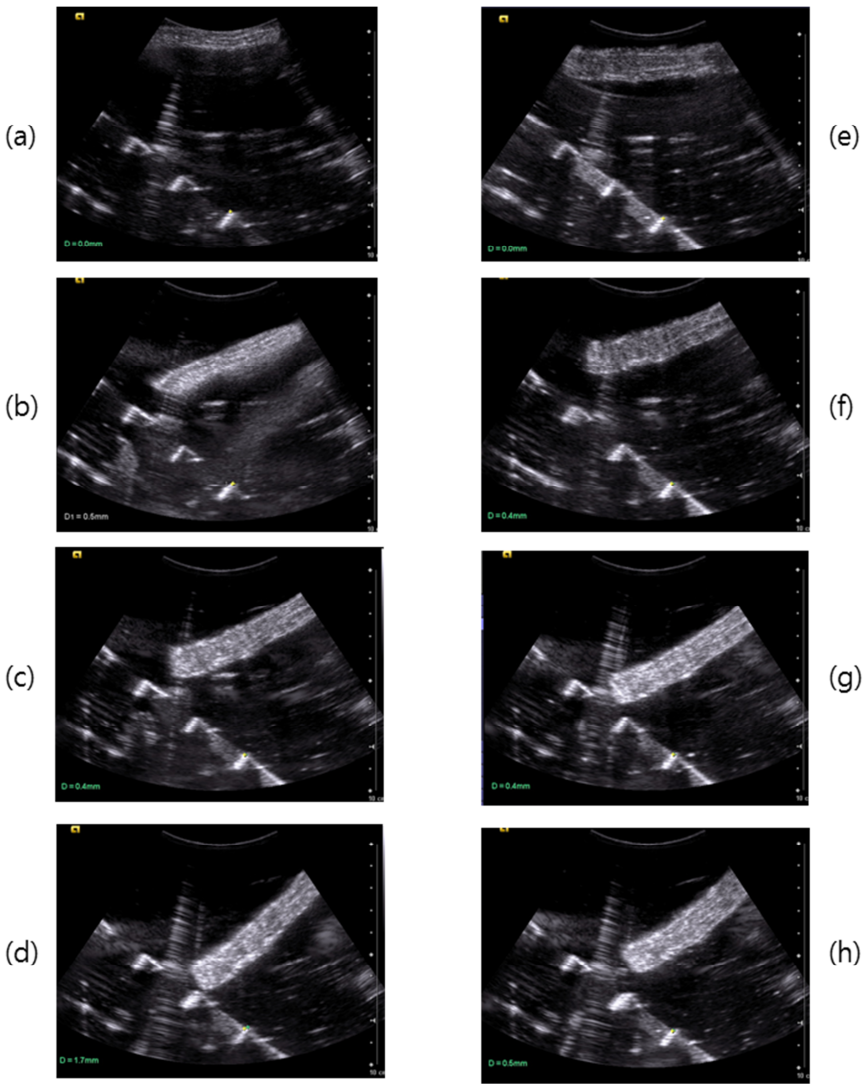

Figure 5.4 Distortion experiment images with different incident angles. (a) Fat **0°** (b) Fat **15°** (c) Fat 30° (d) Fat 4**5°** (b) Muscle **0°** (f) Muscle **15°** (g) Muscle 30° (h) Muscle **45°**

Table 5.1 The errors caused by refraction of the fat and muscle phantoms at different angles.

Incident angle	Fat phantom [mm]	Muscle phantom [mm]
0°	< 0.1	< 0.1
15°	0.3	0.4
30°	0.4	0.5
45°	1.7	0.8

Beam Thickness

I examined the localization error caused by beam thickness. The average experimental error among the technicians was 0.42 ± 0.29 mm. This includes diffused reflection error inherent to ultra-sound systems.

Effect and dimensions of errors

Table 5.2 Ultrasound distortion errors and dimension

Kind of Distortion	Error	Dimension
Diffused Refelction	0.3~0.45 mm	x-y
Thickness	0.2~0.6 mm	z
Refraction	< 0.1 mm	x-y-z

Table 5.2 shows the amount of errors that caused by each distortion and its dimensions. Since the incident angle of an ultrasound beam in both experiment and real case is usually near $0°$, the refraction error is negligible. When ignore refraction error, possible error caused by ultrasound distortion is 0.36~0.75mm. When we use six fiducial markers, possible FRE caused by ultrasound distortion is 0.306mm calculated by following equation.

$$FRE = \sqrt{\frac{1}{n}\sum_{j=1}^{n}\left|Ti_j - P_j\right|^2}$$

$$FRE_{ud} = \sqrt{\frac{1}{n}error^{\ 2}}$$

In Figure 5.2, maximum different between experiments is 0.795mm which include ultrasound distortion and calibration error. In the ultrasound distortion experiments, the amount of ultrasound error was studied as 0.306mm. Thus, the calibration error can be calculated as 0.489mm. Since ultrasound was used during calibration procedure, the calibration error can include ultrasound distortion error.

Ⅵ. Discussion

The phantom experiment confirmed that registration accuracy is improved when the additional fiducial points are used. However, the improved accuracy fell short of the expected value because of insufficient calibration and ultrasound distortion. Since determining calibration error without ultrasound distortion is impossible, I examined the ultrasound distortions. Diffused reflection, refraction, and thickness error of ultrasound were studied. These distortions are dependent on the environment, such as frequency, kind of ultrasound transducer, focal length, and medium. Thus, the environment of experiments in this study was set up same as the registration experiment. The result can be different in different experiment environment.

In the diffused reflection experiment I expected to see a relationship between the frequency and the error. However, I was unable to identify a significant relationship. In the resulting images, a difference between different frequencies could not be found, which means the material property and roughness of the surface are more dominant than the frequency in the diffused reflection.

The bone phantom showed a smaller error than the fat phantom in the diffused reflection experiment. Because of material property, the bone phantom more effectively reflects the ultrasound beam than fat phantom. Thus, the boundary image of the bone phantom was clearer than the fat phantom. This result means that using bone as an anatomical landmark will be more accurate than using other tissue when using ultrasound in the human body.

The direction of the error caused by beam thickness is perpendicular to the ultrasound image, and the direction of the error caused by diffused reflection is parallel to the ultrasound image. So the summation of errors should be added by root mean square. The direction of the error caused by refraction may be both perpendicular and parallel to the image. However, error caused by refraction is negligible because the incident angle of the ultrasound beam in ultrasound system is very small.

Due to physical property of ultrasound, it is difficult to use for head and lung surgery. Possible applications are abdominal and spine surgery. Especially, spine has many bony anatomical landmarks, and spine surgery needs very accurate operation. Thus, spine surgery is suitable application for this study.

Ⅶ. Conclusions

In this study, a point based registration method which can include an anatomical landmark as an additional fiducial point using ultrasound system was suggested. The registration accuracy with and without additional points was examined. The phantom experiment confirmed that the registration accuracy is improved when the additional points are used. Due to ultrasound distortion and insufficient calibration, the improved accuracy fell short of the expected value.

In a study of ultrasound distortion, diffused reflection and beam thickness can affect the suggested method. Since the incident angle of an ultrasound beam in both experiment and real case is usually near $0°$, the refraction error is negligible.

If the error caused by the ultrasound distortion and insufficient calibration of the ultrasound probe can be reduced, the patient-image registration will be more accurate.

감사의 글

2 년 이란 대학원 생활을 통하여, 일생을 보냄에 있어 피가 되고 살이 되는 좋은 경험을 많이 하였고, 많은 분들의 따뜻한 관심과 애정 어린 질책 속에 또 다시 한층 성숙해질 수 있었습니다. 진정한 이 시대의 지식인으로서 소양과 자세를 일깨워준 모든 분들께 한 분씩 찾아 뵙지 못하고 이렇게 지면으로나마 감사의 인사를 드리고자 합니다.

우선 연구와 강의로 바쁘신 와중에도 논문이 완성되기까지 자상하게 인도해 주시고 연구방향에 대하여 넓은 안목으로 키워주시며 지도해주신 홍재성 교수님께 감사 드립니다. 항상 연구하시는 모습과 학생들을 향한 자상한 모습은 잊지 못 할 것입니다. 논문 심사를 맡아주신 장평훈 교수님과 문전일 부장님께 감사 드립니다. 논문에 대한 유익한 말씀과 충고가 많은 도움이 되었습니다. 몇 안되었던 학생들의 말에 귀 기울여 주시고 도와주셨던 최홍수 교수님, 문상준 교수님께 감사 드립니다.

입학에서부터 논문이 완성되기 까지 2 년이란 배움의 여정이 힘들지 않고 즐거울 수 있게 해준 로봇공학과 1 기 동기들 모두 고맙습니다. 힘든 일이 있을 때 마다 옆에서 격려해준 병식이 형, 짓궂은 장난도 잘 받아주던 준영이, 똑똑한 상원이, 운동 친구 희진이, 성실한 진호 모두에게 고마움을 전합니다. 연구동 건물 뒤에서 의자에 끈을 묶어 족구 했었던 일은 잊지 못할 것입니다.

연구실 선배가 없어서 고생하고 있을 때 선배처럼 도움을 주신 이현기 박사님, 멀리 큐슈 대학교에서 한국까지 와서 도움을 주었던 병현이 형, 내 문제를 자신의 일처럼 고민하고 해답을 찾을 수 있게 도와주었던 Erkin Gezgin 박사와 Nikunj Arunkumar Bhagat 에게도 감사의 말을 전합니다.

연구실 후배들 현석이, 상서, 대근이, 종호 고맙다. 너희들의 도움이 큰 힘이 되었다. 선배지만 내가 더 많이 배우고 간다. 남은 공부 무사히 잘 마치고 각자의 분야에서 건승하길 진심으로 기원한다. 그리고 프로그래밍 도와준다고 고생한 기동아, 고맙다.

끝으로, 항상 조건 없이 무한한 사랑을 베풀어 주시고 응원해 주신 부모님께 감사 드립니다. 뒤늦게 공부하겠다는 저를 믿음과 사랑으로 응원해 주시고 옳은 선택을 할 수 있도록 인도해 주신 아버지, 항상 타지에 있는 아들을 위해 걱정하고 기도해 주시는 어머니께 깊은 감사의 말씀을 드립니다. 그리고 항상 곁에서 묵묵히 내조해준 사랑하는 여자친구 은정이 에게 이 작은 기쁨을 바칩니다.

이외에 제가 미처 언급하지 못한 고마운 분들이 너무나 많습니다. 그 분들의 이름을 하나 하나 되새기지 못함을 죄송하게 생각 하며, 졸업 후 사회로 나가 어느 곳에서 무엇을 하던, 인생의 선후배로서 그리고 친구로서 많은 관심과 애정을 가지고 저를 지켜 봐주셨던 모든 분들께 부끄럽지 않은 모습으로 훗날 다시 뵐 수 있도록 어디서든 최선을 다하겠습니다.

요 약 문

해부학적 특징점을 이용한 고정밀 환자-영상 정합

영상정합은 수술 내비게이션의 정밀도를 결정하는 중요한 요소이다. 포인트 기반의 환자 영상간 영상정합은 비침습적인 방법으로 흔히 사용되는 방법 중 하나이다. 하지만 포인트 기반의 영상정합을 위한 마커는 환자의 피부에만 부착될 수 있고 영상정합 오차는 표면 마커로부터의 거리에 비례해서 점진적으로 늘어나게 된다. 일반적으로 수술 내비게이션의 대상은 환자의 몸 안에 위치해있는 장기이고, 수술대상 근처에서 높은 정밀도가 요구된다. 만약 환자의 수술 대상 장기의 해부학적 특징점을 포인트 기반 영상정합을 위한 마커로 활용할 수 있다면 수술 목표 부근에서 좀더 정밀한 영상정합을 기대할 수 있을 것이다. 본 연구에서는 해부학적 특징점을 포함하는 있는 포인트 기반의 영상정합 방법을 개발 하고 팬텀 실험을 통하여 제안된 방법의 가능성을 평가 한다.

핵심어: 수술 내비게이션, 영상 정합, 초음파

Publications and Awards

Jaeyeong Park, Jaesung Hong, How can the accuracy of target registration be improved in the point based registration method, Proceeding of the 8th Asian Conference on Computer Aided Surgery(ACCAS2012), p13, 2012

Hyunki Lee, Jaesung Hong, Jaeyeong Park, Nikunj Arunkumar Bhagat, Min Young Kim, Kwang Ill Ko, Automatic Calibration Process Development for Augmented Reality in Minimally Invasive Surgery, Proceeding of the 8th Asian Conference on Computer Aided Surgery(ACCAS2012), p27-28, 2012

Jaeyeong Park, Jaesung Hong, 초음파 영상장치를 이용한 고정밀 환자−영상 간 정합, Korean Society of Medical Robot, p45-46, 2012

Jaeyeong Park, Jaesung Hong, High accuracy target registration method using ultrasonography, Proceeding of the 4th SPENALO International Symposium on Marine and Medical Robotics (SIS2012), p55-58, 2012

Best Paper Award, Jaeyeong Park and Jaesung Hong, High accuracy target registration method using ultrasonography, The 4th SPENALO Internation Symposium on Marine and Medical Robotics (SIS2012), 2012

References

1. Kohan, D. and D. Jethanamest, *Image-guided surgical navigation in otology.* Laryngoscope, 2012. **122**(10): p. 2291-9.
2. Casap, N., A. Wexler, and E. Tarazi, *Application of a surgical navigation system for implant surgery in a deficient alveolar ridge postexcision of an odontogenic myxoma.* J Oral Maxillofac Surg, 2005. **63**(7): p. 982-8.
3. Cossey, A.J. and A.J. Spriggins, *The use of computer-assisted surgical navigation to prevent malalignment in unicompartmental knee arthroplasty.* J Arthroplasty, 2005. **20**(1): p. 29-34.
4. Germano, I.M. and J.V. Queenan, *Clinical experience with intracranial brain needle biopsy using frameless surgical navigation.* Comput Aided Surg, 1998. **3**(1): p. 33-9.
5. Ecker, T.M., M. Tannast, and S.B. Murphy, *Computed tomography-based surgical navigation for hip arthroplasty.* Clin Orthop Relat Res, 2007. **465**: p. 100-5.
6. Costa, D.J. and R. Sindwani, *Advances in surgical navigation.* Otolaryngol Clin North Am, 2009. **42**(5): p. 799-811, ix.
7. Hong, J., et al., *Medical navigation system for otologic surgery based on hybrid registration and virtual intraoperative computed tomography.* IEEE Trans Biomed Eng, 2009. **56**(2): p. 426-32.
8. Nijmeh, A.D., et al., *Image-guided navigation in oral and maxillofacial surgery.* Br J Oral Maxillofac Surg, 2005. **43**(4): p. 294-302.
9. Strauss, G., et al., *[The first clinical use of an Dynamic Registration Tool for Navigation in FESS]*. Laryngorhinootologie, 2012. **91**(3): p. 168-73.

10. West, J.B., et al., *Fiducial point placement and the accuracy of point-based, rigid body registration.* Neurosurgery, 2001. **48**(4): p. 810-6; discussion 816-7.

11. Arun, K.S., T.S. Huang, and S.D. Blostein, *Least-squares fitting of two 3-d point sets.* IEEE Trans Pattern Anal Mach Intell, 1987. **9**(5): p. 698-700.

12. Nottmeier, E.W. and T.L. Crosby, *Timing of paired points and surface matching registration in three-dimensional (3D) image-guided spinal surgery.* J Spinal Disord Tech, 2007. **20**(4): p. 268-70.

13. Nuwan D, B.C., Aaron F, *A surface-based metric for registration error quantification.* Fourth International Conference on Industrial and Information Systems, 2009. **4**.

14. Ledderose, G.J., et al., *Image guided surgery of the lateral skull base: testing a new dental splint registration device.* Comput Aided Surg, 2012. **17**(1): p. 13-20.

15. Metzger, M.C., et al., *Comparison of 4 registration strategies for computer-aided maxillofacial surgery.* Otolaryngol Head Neck Surg, 2007. **137**(1): p. 93-9.

16. Zhang, W., et al., *Effect of fiducial configuration on target registration error in image-guided cranio-maxillofacial surgery.* J Craniomaxillofac Surg, 2011. **39**(6): p. 407-11.

17. Fitzpatrick, J.M., J.B. West, and C.R. Maurer, Jr., *Predicting error in rigid-body point-based registration.* IEEE Trans Med Imaging, 1998. **17**(5): p. 694-702.

18. Hajnal, J.V., D.J. Hawkes, and D.L.G. Hill, *Medical image registration*. Biomedical engineering series. 2001, Boca Raton: CRC Press. 382 p., 8 p. of plates.

19. Hong, J. and M. Hashizume, *An effective point-based registration tool for surgical navigation.* Surg Endosc, 2010. **24**(4): p. 944-8.

20. Lemoigne, Y., et al., *Physics for medical imaging applications*. NATO science series Series II, Mathematics, physics, and chemistry. 2007, Dordrecht: Springer. xvii, 406 p.

21. Sjolie, E., et al., *3D ultrasound-based navigation for radiofrequency thermal ablation in the treatment of liver malignancies.* Surg Endosc, 2003. **17**(6): p. 933-8.

22. Beller, S., et al., *Feasibility of navigated resection of liver tumors using multiplanar visualization of intraoperative 3-dimensional ultrasound data.* Ann Surg, 2007. **246**(2): p. 288-94.

23. Nakamoto, M., et al., *Recovery of respiratory motion and deformation of the liver using laparoscopic freehand 3D ultrasound system.* Med Image Anal, 2007. **11**(5): p. 429-42.

24. Konishi K, N.M., Kakeji Y, Tanoue K, Kawanaka H,Yamaguchi S, Ieiri S, Sato Y, Maehara Y, Tamura S, Hashizume M, *A real-time navigation system for laparoscopic surgery based on three-dimensional ultrasound usingmagneto-optic hybrid tracking configuration.* Int J Comput Assis Radiol Surg, 2007. **2**(1): p. 1-10.

25. Edelman, S.K., *Understanding ultrasound physics : fundamentals and exam review*. 1st ed. 1990, Houston, Tex.: E.S.P. Publishers. 266 p.